HHS Public Access

Author manuscript

Biosens Bioelectron X. Author manuscript; available in PMC 2025 May 06.

Published in final edited form as:

Biosens Bioelectron X. 2025 May ; 23: . doi:10.1016/j.biosx.2025.100593.

A deeper evaluation of cytokeratin fragment 21–1 as a lung cancer tumor marker and comparison of different assays

Dianna J. Rowe[a], **Timothy A. Khalil**[a], **Michael N. Kammer**[a], **Caroline M. Godfrey**[a], **Yong Zou**[a], **Cindy L. Vnencak-Jones**[d], **David Xiao**[a], **Stephen Deppen**[c], **Eric L. Grogan**[b,c,*]

[a]Department of Medicine, Division of Allergy, Pulmonary and Critical Care Medicine, Vanderbilt University Medical Center, Nashville, TN, USA

[b]Tennessee Valley Healthcare Systems, Nashville Campus, Nashville, TN, USA

[c]Department of Thoracic Surgery, Vanderbilt University Medical Center, Nashville, TN, USA

[d]Department of Pathology, Microbiology and Immunology, Vanderbilt University Medical Center, Nashville, TN, USA

Abstract

Studies show CYFRA 21–1 fragments of cytokeratin 19 (CK19) to be promising biomarkers for non-small cell lung cancer (NSCLC). Although previous literature identifies specific CYFRA 21–1 antibody binding epitopes, the exact molecular weight of the CK19 fragment being detected by current assays is not well-documented. Serum samples from 58 patients (lung cancer (N = 36), control (N = 22)) were used to measure CYFRA 21–1 across four different quantification assays: enzyme-linked immunosorbent assay (ELISA), chemiluminescent assay (ChLIA), electrochemiluminescence immunoassay (ECLIA), and compensated interferometric reader (CIR). In the cancer group, correlation between ECLIA and ELISA was high ($R_{(Pearson)}$ = 0.948, $r_{(Spearman)}$ = 0.868) while correlation between ECLIA vs ChLIA and ECLIA vs CIR was low (R= 0.005, r = −0.0593), (R = 0.0275, r = 0.167), respectively. In the control group, correlation between ECLIA and ELISA was high (R = 0.861, r = 0.927) while correlation between ECLIA vs ChLIA and ECLIA vs CIR was low (R = 0.0079, r = −0.0593), (R = 0.0244, r = −0.102), respectively. Compared to ECLIA, concordance coefficients (p_c) were poor ($p_c < 0.90$)

*Corresponding author. Tennessee Valley Healthcare Systems, Nashville Campus, Nashville, TN, USA. eric.grogan@VUMC.org (E.L. Grogan).

Declaration of competing interest

The authors declare that they have no known competing financial interests or personal relationships that could have appeared to influence the work reported in this paper.

CRediT authorship contribution statement

Dianna J. Rowe: Writing – review & editing, Writing – original draft, Methodology, Formal analysis, Data curation. **Timothy A. Khalil:** Writing – review & editing, Writing – original draft, Methodology, Investigation. **Michael N. Kammer:** Writing – review & editing, Supervision, Methodology, Investigation, Data curation, Conceptualization. **Caroline M. Godfrey:** Writing – original draft, Investigation, Funding acquisition, Conceptualization. **Yong Zou:** Resources, Investigation, Data curation. **Cindy L. Vnencak-Jones:** Writing – review & editing, Supervision, Methodology. **David Xiao:** Writing – review & editing, Investigation, Funding acquisition, Conceptualization. **Stephen Deppen:** Writing – review & editing, Supervision, Conceptualization. **Eric L. Grogan:** Writing – review & editing, Project administration, Methodology, Investigation, Funding acquisition, Conceptualization.

Appendix A. Supplementary data

Supplementary data to this article can be found online at https://doi.org/10.1016/j.biosx.2025.100593.

across all assays except for cancers group in ELISA ($\rho_c = 0.913$). ECLIA was the only assay to report control ranges above 1 ng/mL CYFRA 21–1 (ECLIA, 1.14–21.59 ng/mL; ELISA, 0.79–24.26 ng/mL; ChLIA, 0.062–0.691 ng/mL; 0.08–7.68 ng/mL). Differing sizes of the protein being measured by each assay may have a role in the discrepancies observed. Given the different CYFRA 21–1 concentration estimates among assays, further characterization of the fragment and its release during epithelial malignancies, such as NSCLC, is imperative to developing effective biomarker assays.

Keywords

CYFRA 21–1; Biomarker; Enzyme-linked immunosorbent assay (ELISA); Chemiluminescent assay (ChLIA); Electrochemiluminescence immunoassay (ECLIA); Compensated interferometric reader (CIR)

1. Introduction

Cytokeratin fragment 21–1 (CYFRA 21–1) has been studied extensively as a promising circulating biomarker for the early detection, diagnosis, and monitoring of lung cancer and several other epithelial cancers for over two decades (Niklinski et al., 1995; Stieber et al., 1993; van der Gaast et al., 1994). However, despite widespread interest, it has not yet been clinically implemented as a marker in lung cancer in the United States. The biggest barriers to the utilization of this marker have historically been (1) the sensitivity of the assay to accurately quantify the marker at low concentrations, where the discriminatory power of the biomarker is most impactful, and (2) a lack of reproducibility of clinical studies. While the broader community has made great strides towards overcoming the first barrier (Kammer et al., 2019; Kammer et al., 2021a; Lee et al., 2012; Olmsted et al., 2014), the second is a much more challenging problem, due to the heterogeneity of patient populations and clinical situations, but also, more fundamentally, the variation in definition of "CYFRA 21–1." This investigation sought to explore the nature of CYFRA 21–1 by beginning to describe the great variation in the reported origin, nature, molecular weight, and description of what many researchers refer to as CYFRA 21–1.

Lung cancer remains the leading cause of cancer-related deaths in the world. A strong contributor to this fact stems from difficulty in detecting lung cancer at an early stage. Nearly 80% of lung cancer diagnoses are detected at later stages (Jemal et al., 2007). However, as the current recommendations for advanced-stage treatment is an individualized a combination of surgery, chemotherapy, targeted therapy, immunotherapy and radiation therapy often with high operational costs and potential procedural risks warrant investigation to improve early detection and diagnosis of lung cancer (Ettinger et al., 2022). Such investigations include the tumor marker CYFRA 21–1, a fragment of cytokeratin 19 (CK19) released from lung epithelial cells in malignant and non-malignant states. Quantification of CYFRA 21–1 in the context of oral squamous cell carcinoma, thymic carcinoma, and interstitial pulmonary fibrosis have revealed the prognostic value of the biomarker in various disease states (Adusumilli et al., 2023; Molyneaux et al., 2022; Shiiya et al., 2021). Specifically in the context of lung cancer, CYFRA 21–1 has shown promise in

recurrence surveillance in non-small cell lung cancer (NSCLC) (Stieber et al., 1993). High serum CYFRA 21–1 values were reported to correlate with poor prognosis, regardless of administered treatment(Pujol et al., 1993). Recent evidence published suggests that improved sensitivity of CYFRA 21–1 measurement via a compensated interferometric reader (CIR) improves discrimination between controls and early-stage NSCLC, offering promise for CYFRA 21–1 use as an early detection biomarker (Kammer et al., 2021a).

While it is expected that assay characteristics may vary by platform and assay performance is dependent upon the origin, quality, and binding site of the antibody (or other capture/detection molecule methods), it is generally assumed that detection and quantification of a specific target molecule is consistent across all platforms to a reasonable degree. In other words, a sandwich principal assay and a surface-plasmon-resonance-based quantitative assay of the same molecule may differ in linear range, sensitivity, and/or have some disagreement within a reasonable range, but they should quantify the same target and reasonably agree for samples that fall into the overlap between their linear ranges. This is generally the case (Bayoumy et al., 2021; Torlakovic et al., 2020), especially for native proteins. The cases where there is significant disagreement between assay types serve as an invitation to further study why assays show disagreement (Beeg et al., 2021). However, the even more egregious scenario is when the reported target molecule significantly differs across assay types, which can result from situations where the target molecule is produced by an uncontrolled process, such as fragmentation.

In this study, we sought to compare the measured CYFRA 21–1 values across four assays while investigating the biochemical underpinnings of the disagreement between assays. It is not the goal of this study to compare the diagnostic ability of these assays, which has been performed previously on much larger datasets using appropriate clinical cohorts of patient samples (Kammer et al., 2019), but rather to understand the differences between assay results between the various methods.

2. Methods

2.1. Patient samples

Serum samples were collected from prospectively enrolled patients in lung cancer studies at Vanderbilt University Medical Center (Nashville, TN) between the years of 2005–2022 and stored in the Thoracic Biorepository. Sample collection, storage and clinical data extraction were approved under the (IRB#030763 and IRB#101404) and patient consent was obtained before enrollment and sample collection. Fifty-eight patients were selected that met requirements for serum volume availability to adequately run on four separate CYFRA 12–1 detection platforms. Thirty-six patients had a histologically confirmed lung cancer diagnosis. Twenty-two control patients were confirmed to have no prior cancer diagnosis and a negative cancer by histological diagnosis at least two years following the date of sample collection (Table 1). Serum samples were barcoded and stored at −80 °C until the time of analysis for this study. Each sample was barcoded and stored in multiple 250uL aliquots at the time of collection. One aliquot was used to perform each individual assay.

2.2. Detection methods

CYFRA 21–1 concentrations were determined in parallel in samples from 58 patients across four different quantification assays. Separate serum aliquots collected from the same sample collection date were used from each patient. At the time of collection, 1 mL serum samples were processed and separated into 250 μL aliquots. Thus, aliquots run from the same sample collection date underwent only one freeze-thaw cycle before being run on separate assays. Enzyme-linked immunosorbent assays (ELISA) were run on the TM-CYFRA 21–1 ELISA RUO kit (DRG International, Germany) based on the sandwich method following manufacturers protocols using reagents provided in the kit. In individual Microtiter wells coated with anti-CYFRA 21–1 antibody, 50 μL of each sample, 50 μL of assay buffer and 10 μL of enzyme conjugate (anti-CYFRA 21–1 antibody with horseradish peroxidase) were thoroughly mixed for 10 s and incubated at room temperature (RT) for 60 min. Wells were then emptied and briskly washed 3 times with 350 μL of washing solution. Subsequently, 200 μL of substrate solution containing tetramethylbenzidine (TMB) was added to each well and incubated for 15 min at RT. The enzymatic reaction was stopped by adding 100 μL of the stop solution and the absorbance of each well was read by a microtiter plate reader within 10 min of adding the stop solution. Controls and standards for the calibration curve were prepared and run on every plate per manufacturer's protocols. Monoclonal mouse antibodies KS19.1 and BM19.21 were used to detect CYFRA 21–1 in this assay. Samples were run in duplicate and averaged to produce reported concentrations in ng/mL.

Electrochemiluminescence Immunoassays (ECLIA) were run on the automated Elecsys CYFRA 21–1 assay compatible with the cobas e401 analyzer (Roche Diagnostics GmbH, Germany) based on the sandwich method following manufacturer's instructions. Monoclonal mouse antibodies KS19.1 and BM19.21 were used to detect CYFRA 21–1. Samples were run in triplicate and averaged to report CYFRA 21–1 values in ng/mL. Serum sample results were determined via a master standard CYFRA 21–1 curve provided by the cobas e401 analyzer software.

Chemiluminescent assays (ChLIA) were run on the Human CYFRA 21–1 ChLIA Kit (Elabscience, Biotechnology, China) based on the sandwich-ChLIA method following manufacturers protocols using reagents provided in the kit. In individual Microtiter wells coated with polyclonal anti-CYFRA 21–1 antibodies, 100 μL of each sample was added and incubated at RT for 90 min. Each well was emptied and 100 μL of biotinylated detection polyclonal anti-CYFRA 21–1 antibody was promptly added to each well. Samples were gently mixed and incubated for 60 min at RT. Three wash cycles with 350 μL wash buffer were preformed then 100 μL of horseradish peroxidase conjugate was added to each well and incubated for 30 min at RT. Five additional wash cycles were performed with 350 μL wash buffer each, aspirating wells between each wash. Finally, 100 μL of substrate mixture solution was added to each well, incubated for 5 min at RT and covered before being promptly read on the chemiluminescence immunoassay analyzer. Controls and standards for the calibration curve were prepared and run on every plate per manufacturer's protocols. Samples were run in duplicate and averaged to calculate CYFRA 21–1 concentration in pg/mL.

For ELISA and ChLIA, samples were run in two separate cohorts: one cohort of 18 patient samples and a second cohort of 40 patient samples. Serum samples results were determined based on standard curves run on the same plate and same date as the sample cohort.

Free Solution Assays (FSA) were run on Compensated Interferometer Reader (CIR) developed at Vanderbilt University, Nashville TN following previously published workflows (Bornhop et al., 2016; Kammer et al., 2019b). Reference samples were formed by mixing 10 μL of serum sample and 30 μL of PBS. Binding samples were formed by mixing 10 μL of serum sample and 30 μL solution containing probe anti-CYFRA 21–1 antibody (1.5 μg/mL). Samples were incubated at RT using shaking (300 rpm) for 60 min before measurement with FSA-CIR. The probe antibody used was a monoclonal mouse clone xC4-BMI19.21 epitope. Samples were run in triplicate and averaged to report CYFRA 21–1 values in ng/mL. See Table 2 for comparison of detection method antibodies, manufacturers, and assay metrics of quantification.

2.3. Analysis & statistics

R 4.0.3 software was used for statistical analysis. Values for ELISA and ChLIA samples are represented as the average of two measurements, and FSA-CIR and ECLIA as the average of three measurements. Standard curves for ELISA, ChLIA, and FSA-CIR assays were fit using 4-parameter saturation isotherm curve and CYFRA 21–1 concentrations estimated using the drc R package (Chetan et al., 2022). Standard curves and CYFRA 21–1 concentrations for the ECLIA were generated from the Roche cobas e401 analyzer software.

Duplicate and triplicate CYFRA 21–1 estimates were used to calculate the intra-assay coefficient of variability (CV(%)). Pearson and Spearman correlation coefficients (r^2) were calculated between intra-assay estimates (ex. Between duplicate reads) and inter-assay for comparison of CYFRA 21–1 measurement reproducibility within and between assays. Concentrations were converted to ng/mL when comparing inter-assay concentrations. Lin's concordance correlation coefficient (CCC) (p_c) (King et al., 2007) was calculated to test how well CYFRA 21–1 pairs of observations from the three additional assays conform to the gold standard ECLIA assay. Lin's CCC (p_c) measures both precision (p) and accuracy ($C\beta$)(Akoglu, 2018). The range of CCC is 0 to ±1 and interpretation of agreement was determined based on McBride et al. classification(Liao and Lewis, 2000) which states agreement as >0.99 almost perfect; 0.95–0.99 substantial; 0.90–0.95 moderate; and <0.90 poor. The ECLIA assay was determined as the gold standard to back compare each assay to, due to the detection method being certified through the Clinical Laboratory Improvement Amendments (CLIA), the College of American Pathologists (CAP) accreditation programs and FDA approval for clinical use.

2.4. Molecular visualization

The assay manufacturer specifications were evaluated to identify CYFRA 21–1 fragment size. The CK19 amino acid sequence was obtained from the Uniprot database (uniport ID P08727) (Consortium, 2022). The three-dimensional structure of CK19 was obtained from Alphafold (alphafold ID AF-P08727-F1-v4) (Jumper et al., 2021; Varadi et al., 2023). UCSF Chimera was used to visualize the structure, evaluate caspase binding sites, and

calculate molecular weights (UCSF Chimera package from the Resource for Biocomputing, Visualization, and Informatics at the University of California, San Francisco, supported by NIH P41 RR-01081) (Pettersen et al., 2004).

3. Results

3.1. Intra-assay concordance

ELISA: The measured range of CYFRA 21–1 values was 0.2–24.26 ng/mL across all 58 samples and was concentrated to the lower half of the assay's detectable range (manufacturer reported range 0.79–50 ng/mL) (Supplemental Fig. 1:A,C). CYFRA 21–1 values between sample duplicates correlated with an r (Pearson) value of 0.9971 and did not show a difference in sample distribution between duplicates (p = 0.22) (Supplemental Fig. 1:B,D). Five samples did not produce a measurable value. Calculation of intra-assay coefficient of variability yielded a value of 15.3%, just above the desired value of 10% (Reed et al., 2002).

ECLIA: The measured range of CYFRA 21–1 concentration was 1.14–21.59 ng/mL. All samples produced a measurable value. Calculation of intra-assay coefficient of variability between triplicates yielded a value of 2.6%

ChLIA: The measured range of CYFRA 21–1 values was 0.038–0.691 ng/mL across 58 samples. Similarly to ELISA, CYFRA 21–1 values were concentrated to the lower half of the assay's detectable range (manufacturer reported 62.5–4000 pg/mL) (Supplemental Fig. 2:A,C). Duplicate sample CYFRA 21–1 values correlated with an R (Pearson) value of 0.821 and r (Spearman) value of 0.752. No difference in duplicate read concentration was noted (p = 0.35) (Supplemental Fig. 2:B,D).

FSA-CIR: The measured range of CYFRA 21–1 concentration was 0.232–7.18 ng/mL. Concentrations were measured at the lower end of the detectable range (80–10000 pg/mL) *(*Supplemental Figure 3*).* Calculation of intra-assay coefficient of variability between triplicates yielded a value of 9.8%.

3.2. Inter-assay comparisons

The range, mean, and standard deviation of replicates were compared across all assays separately between the cancer and control groups (Fig. 1, Table 3). The following discussion compares all assays back to ECLIA only, however correlation coefficients comparisons of all assays can be found in Table 1. It is evident when comparing the mean CYFRA 21–1 concentrations between ELISA and ECLIA that the ELISA reported lower mean values in both the cancer and control groups (2.60 vs 3.90 and 1.94 vs 3.33 ng/mL, respectively). Additionally, the ELISA reported a higher standard deviation compared to the ECLIA in both the cancer and control groups (0.464 vs 0.059 and 0.320 vs 0.112, respectively). Although the calculated Pearson correlation coefficient was above 0.85 in both groups (0.9486 in cancer and 0.8607 in controls) the concordance coefficient (p_c) was >0.90 only in the cancer group ((p_c) = 0.913), suggesting measured CYFRA 21–1 values were more disconcordant between the ELISA and ECLIA assays in the controls yet showed moderate

strength agreement in cancer samples. Interestingly, the Spearman's correlation coefficient reported improved correlation in controls, but worsened correlation in cancers.

Similarly, to ELISA, the mean of CYFRA 21–1 concentrations measured by FSA-CIR is lower than ECLIA in both the control and cancer groups (1.9 vs 3.9 and 1.54 vs 3.33 ng/mL, respectively). Standard deviation was greater in the FSA-CIR cohorts compared to ECLIA, demonstrating agreater range of measured values. Although the Pearson and Spearman correlations were weak, the concordance coefficient (p_c) was also reported as poor between all assays (controls = 0.0992 and cases = 0.−0.0911). These findings suggest weak correlation between ECLIA and CIR values as well as poor strength agreement between CYFRA 21–1 measurement values at a sample-to-sample level.

The CYFRA 21–1 measurements recorded from the ChLIA assay had the lowest concordance with other assays, with concordance coefficient (p_c) of 0.003 for both control and cancer groups. The overall range reported by ChLIA was almost tenfold lower than the other methods, with a measured range below 1 ng/mL for both controls and cases (0.062–0.691 and 0.038–0.62 ng/mL respectively).

The ECLIA assay was the only assay to report all measured CYFRA 21–1 concentrations above 1 ng/mL for both control and cancer groups (measured ranges of 1.19–21.59 and 1.14–7.33 ng/mL, respectively). All three additional assays reported lower mean ranges and CYFRA 21–1 concentrations compared to ECLIA (Table 3, Fig. 1). Distribution of CYFRA 21–1 concentrations across cancer stage (TNM 8th edition (Rami-Porta et al., 2014)) were also plotted and compared between ECLIA, ELISA and FSA-CIR. Due to the goal of this study and the selection of patient serum samples to be used, performance analytics were not conducted, as the appropriate case:control cohort was not used to properly evaluate clinical sensitivity nor specificity. However, analyte concentration by lung cancer staging can be viewed in Supplemental Fig. 4.

4. Discussion

Despite growing evidence of CYFRA 21–1 utility as a tumor biomarker, it's use as an early detection marker in NSCLC has yet to be effectively supported in a clinical setting. This is in part due to low sensitivity of current commercially available assays and inconsistent data on CYFRA 21–1 fragment length and molecular size being measured in each assay. There is clinical evidence of CYFRA 21–1 use as a tumor biomarker in a variety of malignant and non-malignant disease states alike. Jeong et al. demonstrated increased CYFRA 21–1 levels in thyroid cancer patients with distant metastasis as compared to those without metastasis(Jeong et al., 2021). Additionally, CYFRA 21–1 levels have been demonstrated to be elevated in patients with thymic carcinoma and oral squamous cell carcinoma as compared to those with a benign pathology(Shiiya et al., 2021). CYFRA 21–1 has recently been demonstrated to be elevated in Idiopathic Pulmonary Fibrosis (IPF) patients and correlated with disease progression(Molyneaux et al., 2022). This recent finding gives further insight into the etiology of serum CYFRA 21–1 fragments, demonstrating that CYFRA 21–1 may be a marker of epithelial cell destruction and turnover, a process seen in both malignant and benign disease. Specifically in the context of lung cancer,

CYFRA 21–1 has shown promise in recurrence surveillance in non-small cell lung cancer (NSCLC) where high serum CYFRA 21–1 values correlated with poor prognosis (Stieber et al., 1993). Additionally, CYFRA 21–1 offers promise as an early detection biomarker through a study outlining how improved sensitivity of CYFRA 21–1 measurement via a compensated interferometric reader (CIR) can improve discrimination between controls and early-stage NSCLC (Kammer et al., 2021). Thus, CYFRA 21–1 assays prove important for both diagnosis and surveillance of lung cancer. This study compared the measurement of CYFRA 21–1 between four separate detection methods: ELISA, ECLIA, ChLIA and FSA-CIR. We aim to provide insight into the variation in serum CYFRA 21–1 measurements in the context of lung cancer, indicating the need to further characterize CYFRA 21–1 fragments for development of complimentary and unique CYFRA 21–1 signatures in specific disease states by discussion of three key elements: (1) Detection methods and analytics of each assay; (2) Comparison of serum CYFRA 21–1 measurements across assays; and (3) Discrepancies of protein fragmentation and CYFRA 21–1 production.

4.1. Selected methods of detection for comparison of CYFRA 21–1 measurements

In this study, we utilized four different detection methods to measure CYFRA 21–1.

Enzyme-Linked Immunosorbent Assay (ELISA) relies on an antibody-complex binding to the targeted antigen and inducing color change in the solution, either directly or indirectly. In direct ELISA, the primary antibody targeting the antigen is conjugated with an enzyme that results in color change of the solution that can subsequently be measured to calculate the amount of antigen. In indirect ELISA, the primary antibody targets the antigen, however a secondary antibody complexed to an enzyme (commonly horseradish peroxidase) is then added which binds to the primary antibody and induces a color change. The amount of bound enzyme conjugate is directly proportional to the concentration of CYFRA 21–1 in solution in ng/mL. After administration of substrate solution, the magnitude of color change is measured in optical density (OD) units and is used to quantify CYFRA 21–1 concentrations. The DRG ELISA kit uses an indirect detection method and reports a CYFRA 21–1 lower limit sensitivity of 0.79 ng/mL.

Electrochemiluminescence Immunoassay (ECLIA) is a detection tool relying on light emission from labels on antibodies designed to bind the target molecule. ECLIA is a quantitative method for measuring an antibody based on a change in electrochemistry coupled with chemiluminescence (ECL). Specifically, these labels are designed to emit light when electrochemically stimulated by an electric pulse. The labels are attached to antibodies specific for the binding site on the target molecule. An additional antibody targeted at the antigen is attached to paramagnetic beads that will fixate when a magnetic field is applied, allowing the antigen-antibody complex to be separated from the rest of the solution. ECLIA has a larger linear range as compared to ELISA and therefore requires fewer dilutions. For CYFRA 21–1, ECLIA is reported to have an analytic specificity of 95% and an analytical sensitivity lower limit of 3.3 ng/mL (Barillo et al., 2018).

Chemiluminescent immunoassay (ChLIA) relies on a micro plate pre-coated with antibodies specific to the antigen target. Similarly to ELISA, this reaction can occur indirectly or directly. In direct ChLIA, the primary antibody is labeled with a luminescent

molecule which produces a light response upon binding the antigen. In the indirect method, the immobilized antibodies capture the antigen from the sample and a second acridinium ester-labeled antibody binds the antigen, producing a sandwich effect. The fixated antibody-antigen complex is exposed to an alkaline solution, generating a chemical reaction that produces a flash of light(Cinquanta et al., 2017). Unlike ECLIA which relies on electrical input, ChLIA relies on a chemical reaction to produce chemiluminescence. The Elabscience ChLIA kit reports a CYFRA 21–1 lower limit sensitivity of 37.5 pg/mL.

The antibodies traditionally used to detect CYFRA in immunometric assays such as ELISA and ECLIA bind to both CYFRA 21–1 and full length CK19 and therefore should bind to the two different sized molecules. However, additional detection methods have been trialed that rely on optical detection and therefore quantification may not be based on absolute number of bound biomarker molecules (Table 2).

Free Solution Assay measured by the Compensated Interferometric Reader (FSA-CIR) relies on a label-free, optical detection method which measures change in analyte conformation and hydration upon binding. The CIR uses an interferometric sensor based on a simple optical train consisting of a laser, a capillary tube, and a camera. The laser illuminates the capillary, and the light from this beam is refracted by the capillary tube, producing a series of interference “fringes” whose radial position is dependent on the refractive index of the liquid inside the capillary. Antibody probe is added to one aliquot of patient serum and a refractive index-matched reference solution without antibody is added to another aliquot of the same serum sample. The probe generates a conformational change upon binding of the biomarker in the sample, causing a difference in the refractive index as compared to the reference solution. By comparing the interferometric pattern produced by the sample with and without the antibody, protein biomarker concentrations in the sample drawn into the capillary tube can be quantified (Kammer et al., 2019b). The FSA-CIR shows better analytic sensitivity for CYFRA 21–1 compared to more traditional assays. The lower limit of quantification by FSA-CIR has been demonstrated to be 40 pg/mL as compared to 500 pg/mL by ECLIA (Kussrow et al., 2022). This increased analytic sensitivity has been demonstrated to translate to increased discriminatory power of the test. As this technology continues to develop, this increased discriminatory value potentiates the ability for CYFRA 21–1 to develop into a clinically useful biomarker for lung cancer, specifically early-stage detection(Kammer et al., 2021a).

4.2. Comparison of detection methods

Our results reveal discordant CYFRA 21–1 values when measured by assays using different target antibodies (Fig. 1, Table 3). In this study, the ECLIA Elecsys CYFRA 21–1 (Roche Diagnostics GmbH, Germany) was held as the gold standard to compare CYFRA 21–1 measurements between assays due to its CAP and CLIA accreditation and FDA approval. As previously outlined, the ELISA and ECLIA assays both use the same capture and detection antibodies, KS19.1 and BM19.21, and detect CYFRA 21–1 using a sandwich immunometric approach. There exists a strong positive correlation between ELISA and ECLIA (R (Pearson) = 0.9257, r (Spearman) = 0.8975) suggesting a similar trend in serum CYFRA 21–1 measurements. In addition to a reported strong correlation, ELISA

and ECLIA showed a concordance coefficient (p_c) of 0.913 in the cancer group, indicating moderate agreement between CYFRA 21–1 measurements at a sample-to-sample level. However, the concordance coefficient (p_c) in the control group was 0.685 suggesting poor agreement between the assay when measuring control or normal CYFRA 21–1 values. This indicates that factors such as detection technology, sample prep, and variability in fragment length may impact analyte measurement in non-malignant samples. It is important to note that the concordance coefficient measures not only the agreement between the rank measurements of the sample (like the Pearson R) and trend correlation (like Spearman r), but also how close the trend between measurements is equal to 1. This indicates that though the assays may *correlate*, other factors may impact analyte measurement.

Conversely, the assays using different target antibodies (ChLIA and FSA-CIR), showed poor correlation with ECLIA (R (Pearson) = 0.0068, 0.0259, respectively). Interestingly, the ChLIA assay reported values almost tenfold lower than that of ECLIA (mean values = 0.313 and 3.6 ng/mL, respectively), as well as tenfold lower than ELISA and FSA-CIR. The ChLIA assay uses two polyclonal antibodies for analyte detection, and therefore the analyte specificity may be lower than in methods with monoclonal antibodies, however this should lead to a higher measured concentration, as the assay should be reporting CYFRA 21–1 *and* off target interactions. Manufacturing information from the Human CYFRA 21–1 ChLIA Kit (Elabscience, Biotechnology, China) reported no quality control studies on albumin or immunoglobin cross reactivity.

The FSA-CIR assay reported values in a range comparable to ECLIA, reporting controls as 0.08–7.68 ng/mL and cases as 0.08–4.14 ng/mL. Interestingly, the CIR had lower concordance coefficients (p_c) with ECLIA (0.0992 for controls and −0.0911 for cases). As previously mentioned, it is hypothesized that the interferometer may produce values different than the sandwich ECLIA and ELISA assays. Due to the label-free solution method and quantification of the change in refractive index, the FSA-CIR measurements may be representative of different fragment lengths or molecular weights, which may confer additional disease information or diagnostic potential to the assay.

4.3. Caspase cleavage sites of CK19 do not align with caspase aa target sequences

Cytokeratins (CKs) are a group of filamentous proteins composing the intermediate filaments found in the cytoskeleton of epithelial cells (Bodenmüller, 1995). Cytokeratin 19 (CK19) is a 40 kDa protein composed of 400 amino acids, the smallest of the human keratins. CK19 is known to be expressed in both simple and stratified epithelium, including the epithelium covering the bronchial tree (Barillo et al., 2018), and has been shown to be over-expressed in multiple epithelial carcinomas. There is no clear consensus in the literature on the exact mechanism by which CK19 fragments are released into the serum. It has been hypothesized that CK19 fragments are released from cells undergoing apoptosis and subsequently detected in serum (Barillo et al., 2018). This hypothesis of passive CK19 proteolysis upon cell death is often cited as the primary mechanism of fragment release into serum. However, by inhibiting protein translation and demonstrating the subsequent decrease or elimination of detected CK19, Alix-Panabieres et al. suggest that CK19 release

is perhaps an active process by viable cancer cells and not simply a byproduct of an apoptotic process(Alix-Panabières et al., 2009).

It is believed that during apoptosis, CK19 is cleaved by caspases and resulting fragments are released into the serum. These fragments are the targets for various quantification methodologies using patient serum or plasma samples (Alix-Panabières et al., 2009). One of the resulting fragments, cytokeratin fragment 21 (CYFRA 21–1), is often cited to be cleaved by caspase 3 (Dohmoto et al., 2001), however recent literature suggests that other caspases may additionally act on the fragment (Kumar et al., 2014; Schmeck et al., 2004). A proposed caspase cleavage site is located between amino acids 235 and 238 of its sequence (Dohmoto et al., 2001). Upon cleavage, two fragments are released; the fragment bearing the C-terminus of CK19 is characterized as CYFRA 21–1. Two specific antibodies bind to epitopes localized to the CYFRA 21–1 fragment upstream of the caspase cleavage; KS 19.1 is located at aa 311–335 and BM 19.21 at aa 346–367 (Stigbrand et al., 1998) (Fig. 2).

Although this antibody binding pattern suggests specific targeting of the CYFRA 21–1 fragment, there is no clear consensus on the molecular weight of the CYFRA 21–1 fragment being detected through currently available assays, suggesting that perhaps different assays detect different fragment lengths. Uncertainty around this fragment length stems from the incongruent literature evidence on caspase cleavage of CK19. In regulatory apoptotic mechanisms, executioner caspases-3, −6, and −7 have the capacity of targeting, and thus cleaving, numerous substrates. In the context of CK19 cleavage and production of cytokeratin fragments, previous studies have worked to establish parallels among the wide variety of effector caspase substrates, and to furthermore identify common cleavage sites. Such efforts have resulted in the caspase-3 motif DEXD, where D is Asp, E is Glu, and X is any amino acid (Song et al., 2019; Timmer and Salvesen, 2007). Literature outlines CK19 cleavage by caspase-3 during apoptosis to occur at amino acid cleavage site 235–238 (Alix-Panabières et al., 2009), however the aa sequence in this region does not align with the DEXD cleavage motif. In other words, the DEXD motif is not found in the CK19 protein in the amino acid range of 235–238 and therefore caspase-3 would not likely generate a CYFRA 21–1 fragment with a suggested weight of 18.4 kDa, as previously described(Yu et al., 2017). Alternatively, there is evidence to support cleavage of CK19 by caspase-6, a potent apoptosis-inducer characterized in *Streptococcus pneumoniae* invasion of lung epithelium (Schmeck et al., 2004). Caspase-6 is known to cleave via the motif VEXD which does align with the CK19 cleavage site aa 235–238 (Schmeck et al., 2004). Further incongruency on CYFRA 21–1 molecular weights may be attributed to manufactured detection methods developed in varying CK19 fragment lengths. For example, a Chemiluminescent immunoassay (ChLIA) assay (Elabscience Biotechnology, China) describes the detected CYFRA 21–1 fragment to be the length of amino acids 125–400, producing a fragment of 31.5 kDa. Similarly, an Electrochemiluminescence immunoassay (ECLIA) assay (Roche Diagnostics GmbH, Germany) states a detection of a fragment approximately 30 kDa in molecular weight. Production of an approximately 30 kDa CYFRA 21–1 fragment implies a different cleavage site than caspase-6 (Fig. 3). If cleavage would occur after residue 238 (Asp) as frequently stated (Dohmoto et al., 2001), a CYFRA 21–1 fragment of about 18 kDa should be produced. Contrarily, some CYFRA 21–1 assays do not detect 18 kDa CK19 fragments; the Elecsys CYFRA 21–1 assay (Roche Diagnostics GmbH,

Germany) expects the detection of a 30 kDa CYFRA 21–1 protein (Fig. 3). Hence, the actual size of the protein being measured by each assay may have a role in the differences seen in protein detection.

5. Conclusion

To our knowledge, this is the first study to compare serum CYFRA 21–1 levels in a patient cohort between ECLIA, ELISA, ChLIA and FSA-CIR detection methods. Although the use of CYFRA 21–1 as a biomarker has been investigated in malignant and non-malignant settings, it's utility as a tool for early detection of lung cancer has not yet been effectively demonstrated in a clinical setting. One barrier to widespread clinical validation is the varying results when measuring CYFRA 21–1 across different assay types, including those that purport to measure the same analyte, leading to inconsistent results in the literature about the performance of CYFRA 21–1 as a diagnostic biomarker. In this study, we demonstrated quite discordant results between the four assays, but found these results are potentially explained by assay detection methods and the biochemistry of CYFRA 21–1. Overall, our study reveals discordant CYFRA 21–1 values when measured by assays using different target antibodies (Fig. 1, Table 3). Across all assays, the comparison of cancer groups between ELISA and ECLIA was the only assay comparison that yielded strong positive correlation (R (Pearson) > 0.9) in conjunction with adequate agreement through concordance coefficient (p_c > 0.9). The ELISA and ECLIA assays detect CYFRA 21–1 using similar sandwich methods through capture by the same detection antibodies, KS19.1 and BM19.21. Despite any detection similarities, across all assay comparisons in the control group, no comparisons yielded a strong positive correlation (R (Pearson) > 0.9) nor adequate agreement through concordance coefficient (p_c > 0.9). This indicates that factors such as detection technology, sample prep, and variability in fragment length may impact analyte measurement in non-malignant samples.

Additionally, the discrepancies of CYFRA 21–1 biochemistry contribute to poor concordance in measured serum values. It is established that cytokeratin 19 exists as a 40 kDa molecule and is cleaved by caspases to produce the fragment CYFRA 21–1. These caspase binding sites vary greatly between different literature studies and commercially available detection assays, with reports of CYFRA 21–1 molecular weight varying from 18.4 kDa to 31.5 kDa. Perhaps different caspase activity and resulting variation in fragment length could help define specific CYFRA 21–1 signatures for specific epithelial disease states. Development of new complimentary CYFRA 21–1 assays can potentially widen characterization of these disease states and expand CYFRA 21–1 clinical utility.

Of the methods utilized to detect CYFRA 21–1 in serum, some can discriminate between different molecular sizes, and some are simply detecting antibody concentration, which correspond to the absolute number of molecules bound to the target antibody. The immunometric assays (ECLIA, ELISA and ChLIA) will effectively produce measurements that reflect the absolute value of antibody bound to the target molecule, regardless of whether the antibody is binding full-length CK19 or the resulting CYFRA 21–1 fragments. However, due to the unique sensing paradigm of FSA-CIR, the measurements from FSA-CIR could be due to an increased absolute number of molecules, different changes in

confirmation shape upon antibody binding, or simply larger molecular fragments. Detection methods based on optical detection of confirmation change of antibody binding could yield differences in quantification based on full-length or fragmented protein capture. In other words, the FSA-CIR may be reporting not only different concentrations of CYFRA 21–1, but different fragment lengths or conformations (Bornhop et al., 2016). Different detection paradigms in conjunction with inconsistent data on fragment length and molecular weight of CYFRA 21–1 being detected by these assays likely contribute to discordant values reported here in this study.

5.1. Further investigations

Reconciliation of CYFRA 21–1 discrepancies ultimately depends on the validation of the CK19 protein structure, as well as identification of a molecular pathway defining CK19 cleavage. Although some work has outlined the CK19 conformation, the confidence in the structure of the loop domains specifically remains very low(Jumper et al., 2021; Varadi et al., 2022). Hence, experimentation using mass spectrometry coupled with protein crystallography with nuclear magnetic resonance (NMR) may serve to reduce the uncertainty in the conformation of these domains. Additionally, understanding CK19 conformation may give an indication as to how anti-CYFRA 21–1 antibodies (i.e., KS19.1 and BM19.21) physically bind to the CYFRA 21–1 fragment, and if they have the capability of binding the whole CK19 protein as well.

Additionally, further investigation is essential to properly assess caspase activity on CK19 and the resulting fragmentation. Characterization of differing fragment lengths may help define specific CYFRA 21–1 signatures in epithelial disease states, opening doors of developing new complimentary CYFRA 21–1 assays. In vitro expression and isolation of the full-length CK19 protein would allow for testing of the effects of different caspases (i.e., caspase-3, −6, and −7), as well as determining fragment sizes via immunoblotting. Additionally, identifying and isolating a CK19 fragment would allow for cleavage site determination via sequencing processes such as Edman degradation. Further characterization of the heterogeneity of CK19 fragments may open doors to attribute different fragment lengths to different disease states. Such an example can be seen in the expansion of troponin (cTn) assays for the diagnosis of acute myocardial infarction (Lan and Bell, 2019). This assay has been expanded to include cardiac troponin I (cTnI) and cardiac troponin T (cTnT), specific markers for distinct phases of cardiac infarction and different associations with outcomes (Welsh et al., 2019).

ECLIA was the only assay to report a CYFRA 21–1 range of above 1 ng/mL across all 58 patients (1.19–21.59 and 1.14–7.33 ng/mL for control and cases, respectively). This uncovers the need to study CYFRA 21–1 serum levels in a large cohort representative of a disease-free population. Such studies have been conducted in Chinese and Korean populations. In the Chinese population, a median CYFRA 21–1 value across 3366 participants was reported to be 1.38 ng/mL (Dai et al., 2018). In the Korean population, a median CYFRA 21–1 value was reported as 1.49 ng/mL out of 4096 participants, with the study suggesting CYFRA 21–1 reference intervals (RI) be continuously verified and established in each clinical laboratory (Yoon et al., 2023). However, no such study has been

conducted in other countries, leaving gaps in knowledge of normal CYFRA 21–1 values in populations across the globe. Understanding a normal pattern or distribution of CYFRA 21–1 in the population is imperative to improving the biomarker's utility in NSCLC and other malignant and non-malignant disease states alike.

5.2. Limitations

One limitation of this study is the small patient cohort size (N = 58) and slight male bias (male = 60.1%). Future studies should aim to analyze larger cohorts for broader representation and application of findings. The goal of this study was not to complete a performance study and evaluate different CYFRA 21–1 assays' ability to differentiate between specific NSCLC stages, treatment response, or recurrence rates. Such studies should be conducted to evaluate assay utility in measuring CYFRA 21–1 in specific NSCLC settings. Additionally, this study only evaluated CYFRA 21–1 measurements on four detection platforms; ECLIA, ELISA, ChLIA, and FSA-CIR. Detection methods such as electrochemiluminescence (ECL) coupled to nanocrystals, ring-opening polymerization (ROP), or surface plasma resonance (SPR) (Aydin et al., 2023; Lu et al., 2021; Wang et al., 2016), among others, were not evaluated, nor were CYFRA 21–1 measurements compared between different manufacturing companies' products of the same detection technology.

Overall, this study provides insight into the variation in serum CYFRA 21–1 measurements , indicating the need to further characterize CYFRA 21–1 fragments for development of complimentary and unique CYFRA 21–1 signatures in specific disease states. This is the first work to investigate differences between detection methods for CYFRA 21–1 in the context of lung cancer management to explore potential new avenues for CYFRA 21–1 assay development.

Supplementary Material

Refer to Web version on PubMed Central for supplementary material.

Acknowledgement

We greatly thank Darryl J. Bornhop, PhD and Amanda Kussrow, PhD with the Vanderbilt University Department of Chemistry for their development of the Free-Solution Assay and Compensated Interferometer (FSA-CIR) and additional time, resources and personal provided to train our laboratory to use the CYFRA assay with FSA-CIR.

Funding

This work was supported by NIH (U01CA152662–06) R01CA252964, T32CA106183, and T32HL087738.

Data availability

Data will be made available on request.

References

Adusumilli P, Babburi S, Venigalla A, Benarji KA, Sai SK, Soujanya P, 2023. J. Oral Maxillofac. Pathol. 27 (1), 98–102. [PubMed: 37234320]

Akoglu H, 2018. Turkish journal of emergency medicine 18 (3), 91–93. [PubMed: 30191186]

Alix-Panabières C, Vendrell JP, Slijper M, Pellé O, Barbotte E, Mercier G, Jacot W, Fabbro M, Pantel K, 2009. Breast Cancer Res. 11 (3), R39. [PubMed: 19549321]

Aydin EB, Aydin M, Sezginturk MK, 2023. Mikrochim. Acta 190 (6), 235. [PubMed: 37219635]

Barillo JL, da Silva Junior CT, Silva PS, de Souza JBS, Kanaan S, Xavier AR, de Araujo EG, 2018. Dis. Markers 2018, 2609767. [PubMed: 29854023]

Bayoumy S, Verberk IMW, den Dulk B, Hussainali Z, Zwan M, van der Flier WM, Ashton NJ, Zetterberg H, Blennow K, Vanbrabant J, Stoops E, Vanmechelen E, Dage JL, Teunissen CE, 2021. Alzheimers Res. Ther. 13 (1), 198. [PubMed: 34863295]

Beeg M, Burti C, Allocati E, Ciafardini C, Banzi R, Nobili A, Caprioli F, Garattini S, Gobbi M, 2021. Sci. Rep. 11 (1), 14976. [PubMed: 34294782]

Bodenmüller H, 1995. Scandinavian journal of clinical and laboratory investigation. Supplementum 221, 60–66.

Bornhop DJ, Kammer MN, Kussrow A, Flowers RA 2nd, Meiler J, 2016. Proceedings of the National Academy of Sciences of the United States of America 113 (12), E1595–E1604. [PubMed: 26960999]

Chetan MR, Dowson N, Price NW, Ather S, Nicolson A, Gleeson FV, 2022. Eur. Radiol. 32 (8), 5330–5338. [PubMed: 35238972]

Cinquanta L, Fontana DE, Bizzaro N, 2017. Auto- immunity highlights, 8 (1), 9. [PubMed: 28647912]

Consortium, T.U., 2022. Nucleic acids research 51 (D1), D523–D531.

Dai Y, Qu W, Sang S, Tao S, Li Y, Wang Y, Li Q, Wu T, Zhu A, Chen Q, Song J, Li Q, Ji Y, Zheng Y, Wang F, 2018. Clin. Lab. 64 (1), 123–133. [PubMed: 29479889]

Dohmoto K, Hojo S, Fujita J, Yang Y, Ueda Y, Bandoh S, Yamaji Y, Ohtsuki Y, Dobashi N, Ishida T, Takahara J, 2001. Int. J. Cancer 91 (4), 468–473. [PubMed: 11251967]

Ettinger DS, Wood DE, Aisner DL, Akerley W, Bauman JR, Bharat A, Bruno DS, Chang JY, Chirieac LR, D'Amico TA, DeCamp M, Dilling TJ, Dowell J, Gettinger S, Grotz TE, Gubens MA, Hegde A, Lackner RP, Lanuti M, Lin J, Loo BW, Lovly CM, Maldonado F, Massarelli E, Morgensztern D, Ng T, Otterson GA, Pacheco JM, Patel SP, Riely GJ, Riess J, Schild SE, Shapiro TA, Singh AP, Stevenson J, Tam A, Tanvetyanon T, Yanagawa J, Yang SC, Yau E, Gregory K, Hughes M, 2022. J. Natl. Compr. Cancer Netw. : J. Natl. Compr. Cancer Netw 20 (5), 497–530.

Jemal A, Siegel R, Ward E, Murray T, Xu J, Thun MJ, 2007. CA: a cancer journal for clinicians 57 (1), 43–66. [PubMed: 17237035]

Jeong C, Lee J, Yoon H, Ha J, Kim MH, Bae JS, Jung CK, Kim JS, Kang MI, Lim DJ, 2021. Cancers 13 (4).

Jumper J, Evans R, Pritzel A, Green T, Figurnov M, Ronneberger O, Tunyasuvunakool K, Bates R, Žídek A, Potapenko A, Bridgland A, Meyer C, Kohl SAA, Ballard AJ, Cowie A, Romera-Paredes B, Nikolov S, Jain R, Adler J, Back T, Petersen S, Reiman D, Clancy E, Zielinski M, Steinegger M, Pacholska M, Berghammer T, Bodenstein S, Silver D, Vinyals O, Senior AW, Kavukcuoglu K, Kohli P, Hassabis D, 2021. Nature 596 (7873), 583–589. [PubMed: 34265844]

Kammer M, Kussrow A, Webster R, Chen H, Hoeksema M, Christenson R, Massion P, Bornhop D, 2019. Acs combinatorial. Science 21 (6), 465–472.

Kammer MN, Lakhani DA, Balar AB, Antic SL, Kussrow AK, Webster RL, Mahapatra S, Barad U, Shah C, Atwater T, Diergaarde B, Qian J, Kaizer A, New M, Hirsch E, Feser WJ, Strong J, Rioth M, Miller YE, Balagurunathan Y, Rowe DJ, Helmey S, Chen SC, Bauza J, Deppen SA, Sandler K, Maldonado F, Spira A, Billatos E, Schabath MB, Gillies RJ, Wilson DO, Walker RC, Landman B, Chen H, Grogan EL, Barón AE, Bornhop DJ, Massion PP, 2021. Am. J. Respir. Crit. Care Med. 204 (11), 1306–1316. [PubMed: 34464235]

King TS, Chinchilli VM, Carrasco JL, 2007. Stat. Med. 26 (16), 3095–3113. [PubMed: 17216594]

Kumar S, van Raam BJ, Salvesen GS, Cieplak P, 2014. PLoS One 9 (10), e110539. [PubMed: 25330111]

Kussrow AK, Kammer MN, Massion PP, Webster R, Bornhop DJ, 2022. ACS Omega 7 (36), 31916–31923. [PubMed: 36120008]

Lan NSR, Bell DA, 2019. The Clinical biochemist. Reviews 40 (4), 201–216.

Lee HJ, Kim YT, Park PJ, Shin YS, Kang KN, Kim Y, Kim CW, 2012. J Thorac Cardiov Sur 143 (2), 421–U447.

Liao JJ, Lewis JW, 2000. PDA J. Pharm. Sci. Technol 54 (1), 23–26.

Lu J, Hao L, Yang F, Liu Y, Yang H, Yan S, 2021. Anal. Chim. Acta 1180, 338889. [PubMed: 34538315]

Molyneaux PL, Fahy WA, Byrne AJ, Braybrooke R, Saunders P, Toshner R, Albers G, Chua F, Renzoni EA, Wells AU, Karkera Y, Oballa E, Saini G, Nicholson AG, Jenkins RG, Maher TM, 2022. Am. J. Respir. Crit. Care Med. 205 (12), 1440–1448. [PubMed: 35363592]

Niklinski J, Furman M, Rapellino M, Chyczewski L, Laudanski J, Oliaro A, Ruffini E, 1995. The journal of. Cardiovasc. Surg 36 (5), 501–504.

Olmsted IR, Hassanein M, Kussrow A, Hoeksema M, Li M, Massion PP, Bornhop DJ, 2014. Analytical chemistry 86 (15), 7566–7574. [PubMed: 24954171]

Pettersen EF, Goddard TD, Huang CC, Couch GS, Greenblatt DM, Meng EC, Ferrin TE, 2004. J. Comput. Chem. 25 (13), 1605–1612. [PubMed: 15264254]

Pujol JL, Grenier J, Daurès JP, Daver A, Pujol H, Michel FB, 1993. Cancer Res. 53 (1), 61–66. [PubMed: 7677981]

Rami-Porta R, Bolejack V, Giroux DJ, Chansky K, Crowley J, Asamura H, Goldstraw P, 2014. J. Thorac. Oncol. : official publication of the International Association for the Study of Lung Cancer 9 (11), 1618–1624.

Reed GF, Lynn F, Meade BD, 2002. Clinical and diagnostic laboratory immunology, 9 (6), 1235–1239. [PubMed: 12414755]

Schmeck B, Gross R, N'Guessan PD, Hocke AC, Hammerschmidt S, Mitchell TJ, Rosseau S, Suttorp N, Hippenstiel S, 2004. Infect. Immun. 72 (9), 4940–4947. [PubMed: 15321985]

Shiiya H, Ujiie H, Hida Y, Kato T, Kaga K, Wakasa S, Kikuchi E, Shinagawa N, Okada K, Ito YM, Matsuno Y, 2021. Thoracic cancer 12 (21), 2933–2942. [PubMed: 34581013]

Song J, Wang Y, Li F, Akutsu T, Rawlings ND, Webb GI, Chou KC, 2019. Brief Bioinform 20 (2), 638–658. [PubMed: 29897410]

Stieber P, Hasholzner U, Bodenmüller H, Nagel D, Sunder-Plassmann L, Dienemann H, Meier W, Fateh-Moghadam A, 1993. Cancer 72 (3), 707–713. [PubMed: 7687515]

Stigbrand T, Andrés C, Bellanger L, Bishr Omary M, Bodenmüller H, Bonfrer H, Brundell J, Einarsson R, Erlandsson A, Johansson A, Leca JF, Levi M, Meier T, Nap M, Nustad K, Seguin P, Sjödin A, Sundström B, van Dalen A, Wiebelhaus E, Wiklund B, Arlestig L, Hilgers J, 1998. Tumour biology : the journal of the international society for oncodevelopmental. Biol. Med. 19 (2), 132–152.

Timmer JC, Salvesen GS, 2007. Cell Death Differ. 14 (1), 66–72. [PubMed: 17082814]

Torlakovic E, Lim HJ, Adam J, Barnes P, Bigras G, Chan AWH, Cheung CC, Chung J-H, Couture C, Fiset PO, Fujimoto D, Han G, Hirsch FR, Ilie M, Ionescu D, Li C, Munari E, Okuda K, Ratcliffe MJ, Rimm DL, Ross C, Røge R, Scheel AH, Soo RA, Swanson PE, Tretiakova M, To KF, Vainer GW, Wang H, Xu Z, Zielinski D, Tsao M-S, 2020. Mod. Pathol. 33 (1), 4–17. [PubMed: 31383961]

van der Gaast A, Schoenmakers CH, Kok TC, Blijenberg BG, Cornillie F, Splinter TA, 1994. Br. J. Cancer 69 (3), 525–528. [PubMed: 7510117]

Varadi M, Anyango S, Deshpande M, Nair S, Natassia C, Yordanova G, Yuan D, Stroe O, Wood G, Laydon A, Žídek A, Green T, Tunyasuvunakool K, Petersen S, Jumper J, Clancy E, Green R, Vora A, Lutfi M, Figurnov M, Cowie A, Hobbs N, Kohli P, Kleywegt G, Birney E, Hassabis D, Velankar S, 2022. Nucleic Acids Res. 50 (D1), D439–d444. [PubMed: 34791371]

Varadi M, Bertoni D, Magana P, Paramval U, Pidruchna I, Radhakrishnan M, Tsenkov M, Nair S, Mirdita M, Yeo J, Kovalevskiy O, Tunyasuvunakool K, Laydon A, Žídek A, Tomlinson H, Hariharan D, Abrahamson J, Green T, Jumper J, Birney E, Steinegger M, Hassabis D, Velankar S, 2023. Nucleic acids research 52 (D1), D368–D375.

Wang H, Wang X, Wang J, Fu W, Yao C, 2016. Sci. Rep. 6, 33140. [PubMed: 27615417]

Welsh P, Preiss D, Hayward C, Shah ASV, McAllister D, Briggs A, Boachie C, McConnachie A, Padmanabhan S, Welsh C, Woodward M, Campbell A, Porteous D, Mills NL, Sattar N, 2019. Circulation 139 (24), 2754–2764. [PubMed: 31014085]

Yoon S, Lim YK, Kim HR, Lee MK, Kweon OJ, 2023. Annals of laboratory medicine 43 (1), 82–85. [PubMed: 36045060]

Yu Z, Zhang G, Yang M, Zhang S, Zhao B, Shen G, Chai Y, 2017. Oncotarget 8 (3), 4043–4050. [PubMed: 28008142]

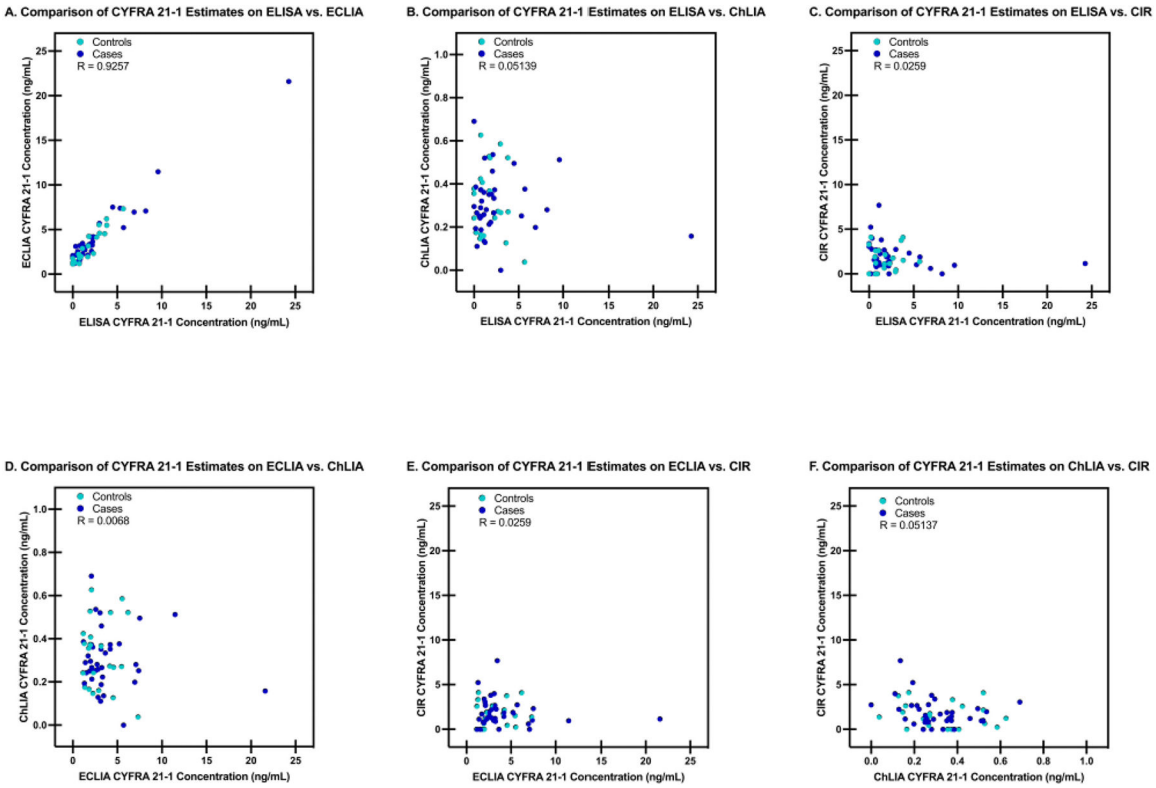

Fig. 1. Scatterplot of inter-assay comparisons of ELISA, ECLIA, ChLIA and CIR.

The R value refers to calculated Pearson correlation coefficient. (ELISA: Enzyme-Linked Immunoassay. ECLIA: Electrochemiluminescence Assay. ChLIA: Chemiluminescent Immunoassay. FSA-CIR – Free Solution Assay measured by the Compensated Interferometric Reader.)

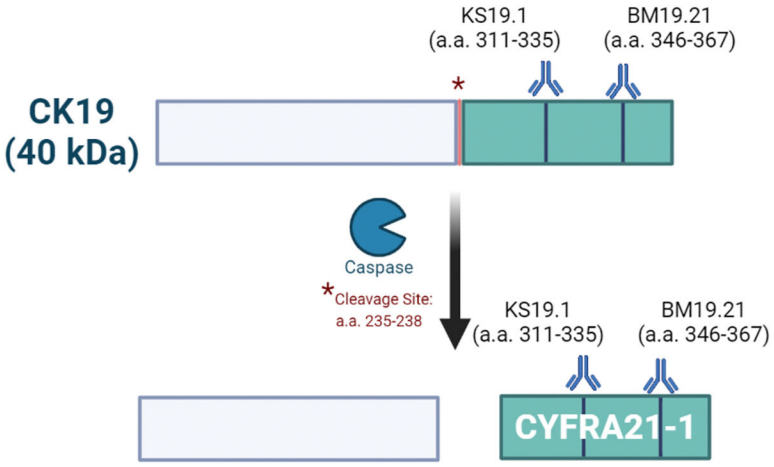

Fig. 2. Schematic of cytokeratin 19 structure and select commercial antibody binding sites.

Two antibodies are known to bind specifically to the amino acid sequences upstream of the caspase cleavage site. KS19.1 binds at amino acids 311–355 and BM19.21 binds at amino acids 346–358. Cytokeratin 19 (CK19) is known to be 40 kDa, however there is no consensus on the molecular weight of the fragments produced upon cleavage. CK19 cleaved at amino acids 235–238 produces a fragment CYFRA 21–1 (Created with biorender.com).

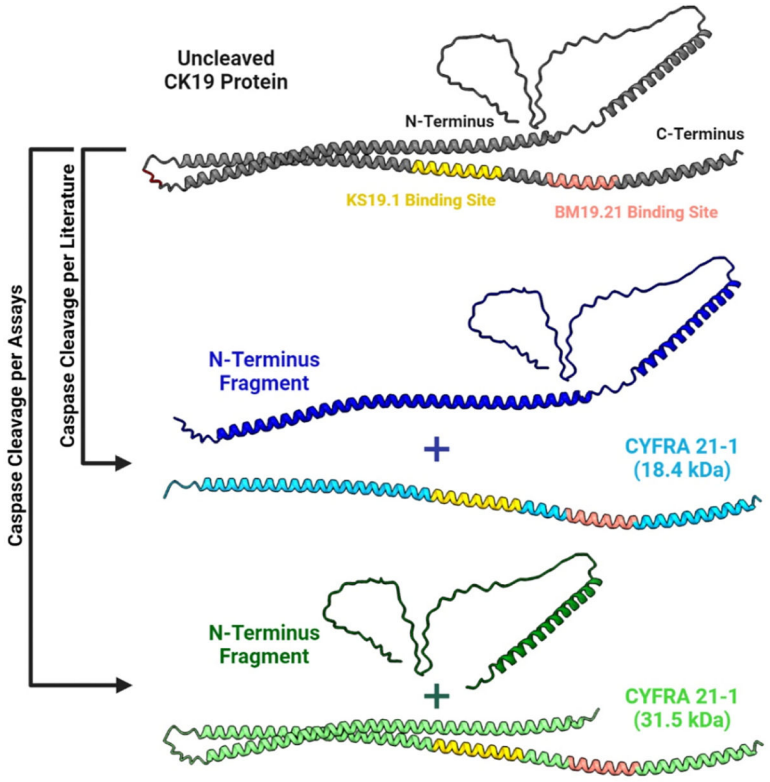

Fig. 3. Cytokeratin 19 structure and resultant fragment lengths from different cleavage sites.
Uncleaved CK19 is known to have a molecular weight of 40 kDa (grey protein). The antibody binding epitopes of KS19.1 and BM19.21 remain on the C-terminus fragment regardless of cleavage site. Caspase cleavage by caspase-6 suggests a CYFRA 21–1 fragment production of 18.4 kDa (blue protein). CYFRA 21–1 molecular weight as proposed by commercially available assays suggests a CYFRA 21–1 fragment of 31.5 kDa (green protein). (Created with biorender.com and chimera.com).

Table 1 Summary of CYFRA 21-1 Detection Methods Used in Inter-Assay Comparison:

ELISA and ECLIA both use antibodies with epitopes KS19.1 and BM19.21 to detect CYFRA 21-1 via a sandwich method. CIR uses an antibody with a shared epitope of ELISA and ECLIA, but only uses one antibody during detection. ChLIA also uses a sandwich method of detection, however, uses polyclonal antibodies with no known epitope information. Normal CYFRA 21-1 values describe the cut-off recommended by the assay manufacturer to differentiate between elevated CYFRA 21-1 levels and normal values.

	ELISA	ECLIA	ChLIA	FSA-CIR
Assay Manufacturer	DRG Instruments	Roche Diagnostics	Elabscience	Vanderbilt University
Volume of Sample Loaded	50 μL	100 μL	100 μL	0.75 μL
Antibody Types	Monoclonals (mouse) KS19.1 and BM19.21	Monoclonals (mouse) KS19.1 and BM19.21	Polyclonal (mouse, capture) and Polyclonal (rabbit, detection)	Monoclonal (mouse) Clone XC4, (BM19.21 like) MyBioSource
Reportable Range (CYFRA 21-1 Concentration)	0.79–50 ng/mL	0.5–100 ng/mL	0.06–4 ng/mL	0.08–10 ng/mL
Limit of Quantification (LOQ)	0.79 ng/mL	0.5 ng/mL	0.062 ng/mL	0.08 ng/mL
Limit of Detection (LOD)	0.185 ng/mL	0.3 ng/mL	0.038 ng/mL	0.003 ng/mL

(LOQ: Limit of Quantification. LOD: Limit of Detection. ELISA: Enzyme-Linked Immunoassay. ECLIA: Electrochemiluminescence Assay. ChLIA: Chemiluminescent Immunoassay. FSA-CIR – Free Solution Assay measured by the Compensated Interferometric Reader.)

Table 2 Patient demographics stratified by lung cancer status.

Age reported in years. Smoking defined as current smoker if smoked within at least one year of sample collection date. Staging reported as TMN Version 8.

	No Cancer (N = 22)	Cancer (N = 36)	All Patients (N = 58)
Age (mean ± STDEV)	67.31 ± 9.31	68.18 ± 8.55	67.47 ± 8.93
Gender (%)			
Male	13 (59.1)	22 (61.1)	35 (60.3)
Female	9 (40.9)	14 (38.9)	23 (39.7)
Race			
African American	1 (4.5)	3 (3.8)	4 (6.9)
Asian	1 (4.5)	0 (0)	1 (1.7)
Caucasian	20 (91)	33 (91.7)	53 (91.4)
Smoking (%)			
Current Smoker	11 (50)	12 (33.3)	23 (39.7)
Former Smoker	10 (45.5)	19 (52.8)	29 (50)
Never Smoked	1 (4.5)	2 (5.6)	3 (5.2)
NA	0 (0)	3 (8.3)	3 (5.2)
Pack Years (mean ± STDEV)	64.43 ± 31.50	62.74 ± 30.08	63.26 ± 30.12
Staging (%)			
I	0 (0)	17 (47.2)	17 (29.3)
II	0 (0)	13 (36.1)	13 (22.4)
III & IV	0 (0)	6 (16.7)	6 (10.3)

Table 3

Inter-assay comparisons of ELISA, ECLIA, ChLIA and CIR.

Cancer (N=36)				
	ECLIA	**ELISA**	**ChLIA**	**CIR**
Range (ng/mL)	1.19–21.59	0.79 *–24.26	0.062 *–0.691	0.08 *–7.68
Mean (ng/mL)	3.9	2.6	0.3	1.9
Standard Deviation (ng/mL)	0.059	0.464	0.083	0.742
† **Concordance Coefficient (p_c)**		0.913	−0.003	−0.0911
† **R (Pearson) value**		0.948	0.005	0.0275
† **r (Spearman) value**		0.868	−0.0593	0.197
Controls (N=22)				
Range (ng/mL)	1.14–7.33	0.79 *–5.68	0.038–0.62	0.08 *–4.14
Mean (ng/mL)	3.33	1.94	0.326	1.54
Standard Deviation (ng/mL)	0.112	0.32	0.14	0.872
† **Concordance Coefficient (p_c)**		0.686	−0.003	0.0992
† **R (Pearson) value**		0.861	0.0079	0.0244
† **r (Spearman) value**		0.927	−0.0593	−0.102

Overall, all three assays (ELISA, ChLIA and CIR) report a concentration range lower than ECLIA. Mean values between ELISA and ECLIA between cancer and controls report a lower value for all three assays compared to the ECLIA assay.

* Values recorded as ‘0.0’ are reported as the Limit of Detection (LOD).

** Concordance compared to ECLIA, calculated using Lin’s concordance correlation coefficient (CCC) (p_C) (King, Chinchilli et al., 2007).

† Values compared to Roche ECLIA across all assays.

(ELISA – Enzyme-Linked Immunoassay, ECLIA – Electrochemiluminescence Assay, ChLIA – Chemiluminescent Immunoassay, CIR – Compensated Interferometric Reader).